EXPERIMENTAL STUDY OF ULTRASONIC VELOCITY AND ANISOTROPY IN COAL SAMPLES

SHOUHUA DONG[1], HAIBO WU[1], DONGHUI LI[2] and YAPING HUANG[1]

[1] *School of Resources and Geosciences, China University of Mining and Technology, Xuzhou 221116, P.R. China. wuhaibocumt@163.com; zywt@cumt.edu.cn*
[2] *School of Safety Science and Engineering, Henan Polytechnic Univ., Jiaozuo 454000, P.R. China.*

(Received April 24, 2015; revised version accepted December 7, 2015)

ABSTRACT

Dong, S., Wu, H., Li, D. and Huang, Y., 2016. Experimental study of ultrasonic velocity and anisotropy in coal samples. *Journal of Seismic Exploration*, 25: 131-146.

Measurements of ultrasonic velocities in coal samples have been limited until recently. In this study, we collected anthracite samples with high mechanical strength from the Qinshui Basin, China, and measured their ultrasonic velocities perpendicular, parallel, and at 45° to the bedding planes under triaxial stress conditions. Considering the depositional features of coal, combined with observations of the coal block, microscopic observations of the bedding, and analyses of the qS wave velocities, we approximated the samples as vertical transverse isotropy (VTI) media. Subsequently, the calculation of anisotropic coefficients demonstrated that the test samples have weak anisotropy with anisotropic coefficients < 0.2. Additionally, the variations of ultrasonic velocities and anisotropic coefficients under various confining pressures were analyzed. The confining pressure has a critical value below which the ultrasonic velocities increase and the anisotropic coefficients decrease significantly, which corresponds to the dynamic process of microfracture closure. The velocities and anisotropic coefficients change minimally and tend to be constant when the confining pressure is greater than the critical value, exhibiting the characteristics of the mineral matrix. Additionally, this critical value is affected by the axial stress and the coal type. Specifically, different axial pressures were set in this study, and the results illustrate this feature unambiguously. Finally, the data and results from this experiment may provide a reference for further rock physics research into coalbed methane.

KEY WORDS: coal sample, confining pressure, ultrasonic velocity, VTI media, anisotropy.

INTRODUCTION

The Qinshui basin, China, is a favorable area for exploitation as it contains coalbed methane (CBM) resources and developmental fractures in its major reservoirs. Unfortunately, only limited data on the reservoir rock physics

0963-0651/16/$5.00

are available, seriously restricting the exploration and exploitation potential of the CBM. Theoretically, a CBM molecule is absorbed on the internal surface of the matrix (Liu, 2009), and seepage occurs in the reservoirs' microfracture systems after desorption, which shows that this process is closely linked to the microfracture characteristics. These microfracture characteristics, including the orientation and density, are manifested as seismic anisotropy. Therefore, by studying the anisotropic characteristics of coal, we can indirectly achieve better understanding of the microfracture characteristics, allowing the migration and seepage of CBM to be studied. Previous studies have shown that three main factors control the anisotropy of coal: the different orientations of mineral compositions, bedding due to deposition, and microfractures resulting from geo-stress (Wang, 2002; Yu et al., 1991, 1993; Morcote et al., 2010). Under low pressure conditions, the anisotropy is influenced by all three factors. Under high pressure conditions, the microfractures become uniformly oriented and begin to close, so anisotropy is predominantly controlled by the other two factors. Furthermore, under increasing stress, there is no obvious change in the mineral matrix, but significant variations are seen in the microfractures and bedding (e.g., orientation, aspect ratio, density). Therefore, a close relationship between seismic anisotropy and microfracture and bedding characteristics in coal can be assumed.

Dong (2008) conducted an anisotropy measurement of gas coal under normal temperatures and pressures, which showed that the elastic anisotropy of gas coal potentially has the capacity to reveal the orientation and density of microfractures. Wang et al. (2012) measured the ultrasonic velocities in six different types of coal samples, and analyzed the relationship between P-wave and S-wave velocities, as well as density. Yu et al. (1991, 1993) tested the ultrasonic velocities and analyzed the anisotropy of both dry and water-saturated coal samples under stress conditions. Castagna (1993) measured and analyzed the velocity anisotropy of bituminous coal samples. Yao and Han (2008) tested the ultrasonic velocities and anisotropy in two different types of coal samples, and Morcote et al. (2010) conducted a test with six different coal types, and showed that velocity anisotropy was dependent on the coal type. However, these studies mainly focused on the test conditions and environment, as well as the coal type, with limited attention paid to the relationship between anisotropy and microfractures.

In this study, we analyzed coal blocks collected from the Qinshui basin. All samples tested were dry, and we measured the qP wave and qS wave velocities in the samples under triaxial stress and normal temperature conditions. Thereafter, we approximated the samples as vertical transverse isotropy (VTI) media, and calculate the anisotropic coefficients. Finally, we analyzed the variations in the ultrasonic velocities and anisotropic coefficients under various confining pressures.

METHODS

Collection and preparation of coal samples

All the coal samples were collected from the Shihe coal field, on the southeastern edge of the Qinshui basin in China. They were buried at depths of 350-500 m, and were high quality anthracite samples with high mechanical strength. We cut ten cube-shaped coal blocks along the direction parallel to the bedding planes, with lengths of about 300 mm. The samples were then transported to the laboratory after being sealed. Since we could not test these original coal blocks directly, cylindrical samples 100 mm long with diameters of 50 mm were obtained along three orientations: perpendicular, parallel, and at 45° to the bedding planes, as shown in Fig. 1. We prepared eleven groups

(a) Cylindrical coal samples

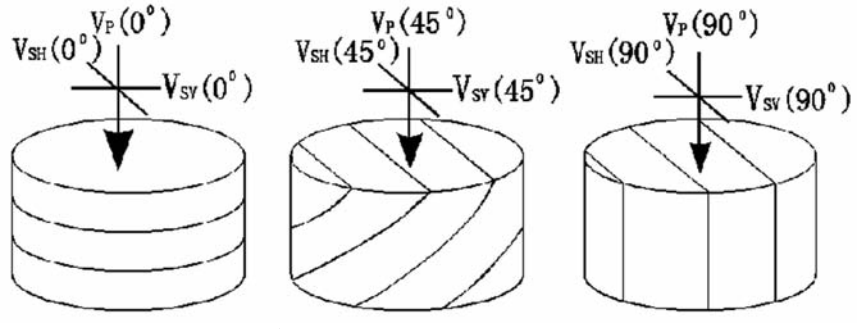

(b) Three types of samples taken at different angles to bedding planes

Fig. 1. Coal samples and schematic diagram for the ultrasonic wave velocity test.

of coal samples, each group consisting of three samples of different orientations from one coal block. Before testing, the samples were left to dry at room temperature for at least 72 hours.

Coal sample porosity and microfracture and bedding descriptions

Porosity tests were conducted under normal temperature and pressure conditions using a type 9310 mercury porosimeter from Micromeritics Instrument Corporation, with a normal working pressure of 0.0028-103.08 MPa. The highest pressure applied to the coal samples was greater than the in situ pressure. The resolution of pore diameter recognition was 0.01 μm. The development and filling of the bedding and microfractures were observed, and are described in Table 1. The porosity of the samples was very limited in range, from 3.09% to 5.08%. The development of the bedding and microfractures differs; for example, filling by calcite (in total or in part) was generally seen only in the bedding.

Table 1. Porosity and characterization of bedding and microfractures of coal samples.

Coal Sample Group	Porosity	Bedding & Fillings Observation & Description	Fractures Observation & Description	Lithotype
1	4.94%	Thin vein calcite partial filling	Developed	Grance Coal
2	4.54%	Vein calcite filling	Developed	Grance Coal
3	5.08%	Vein calcite filling	Undeveloped	Grance Coal
4	4.63%	Vein calcite partial filling	Moderate	Grance Coal
5	4.70%	Thin vein calcite partial and short filling	Moderate	Grance Coal
6	3.39%	Vein calcite partial filling	Undeveloped	Grance Coal
7	4.63%	Thin vein calcite partial and short filling	Undeveloped	Grance Coal
8	4.73%	Vein calcite filling	Developed	Grance Coal
9	3.09%	Vein calcite partial filling	Moderate	Grance Coal
10	4.91%	Thin vein calcite partial and short filling	Moderate	Grance Coal

Ultrasonic velocity test

The external triaxial stress was provided by an MTS815 Flex Test GT rock mechanics system, shown in Fig. 2. The axial pressure of this system ranged from 0 to 4600 kN, and the highest confining pressure was 140 MPa. The ultrasonic velocity tests were conducted using a PCI-2 ultrasonic wave emission testing and specification system, produced by PAC Company, with a working frequency range of 1 kHz to 3 MHz. This system can provide several functions, including pulse signal emission, signal transformation, signal amplification with high fidelity, and automatic signal reception and transmission.

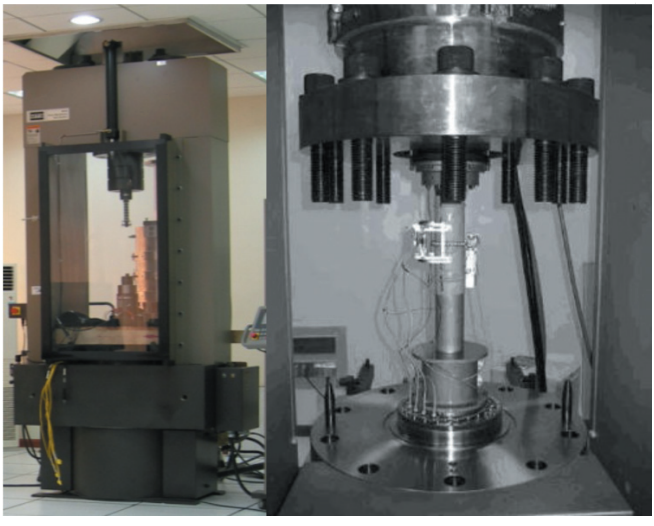

Fig. 2. MTS815 Flex Test GT rock mechanics experimental system.

Before testing, the system was calibrated using an aluminum cylinder under different pressures. Thereafter, the bottoms of the test samples were smeared with a coupling agent and placed vertically between the transducers. The sample was also jacketed with a rubber membrane to isolate it from the fluid that transmits the confining pressure. The ultrasonic wave transmitter and receptor (including one qP wave and two qS wave transducers with a main frequency of 600 kHz and a diameter of 50 mm), as well as the axial displacement gauge (to correct the length of samples under stress), were set between the upper and lower plates. The ultrasonic wave emission used the pulse emission technique (Birch, 1960). For this test, we set three axial pressure levels of 4, 7, and 10 MPa, and six confining pressures of 2, 4, 6, 8, 10, and 12 MPa. Both axial and confining pressures were gradually increased. We recorded the waveform two hours after each pressure was applied.

Table 2. Ultrasonic velocities and anisotropic coefficients of coal samples.

Coal Sample Group	Axial Pressure (MPa)	Confining Pressure (MPa)	Density (g/cm^3)	Ultrasonic Velocities (km/s)									Anisotropy Coefficients		
				Parallel to Bedding (90°)			Angle to Bedding (45°)			Perpendicular to Bedding(0°)					
				qP	qSH	qSV	qP	qSH	qSV	qP	qSH	qSV			
	4	14	1.44	2.334	1.236	1.156	2.304	1.231	1.200	2.280	1.060	1.015	0.024	0.210	0.018
	4	12	1.44	2.310	1.219	1.154	2.278	1.230	1.195	2.244	1.048	1.013	0.030	0.200	0.031
	4	10	1.44	2.284	1.194	1.153	2.262	1.228	1.191	2.222	1.030	1.000	0.028	0.192	0.045
	4	8	1.44	2.268	1.177	1.149	2.234	1.220	1.183	2.155	1.013	0.991	0.054	0.190	0.099
	4	6	1.44	2.250	1.174	1.148	2.195	1.206	1.176	2.079	1.009	0.980	0.086	0.197	0.152
	4	4	1.44	2.233	1.172	1.147	2.139	1.196	1.158	2.028	0.997	0.969	0.106	0.211	0.121
	4	2	1.44	2.192	1.154	1.115	2.083	1.181	1.142	1.976	0.960	0.936	0.115	0.241	0.106
1	4	0	1.44	2.162	1.158	1.111	1.952	1.168	1.131	1.869	0.935	0.902	0.169	0.295	-0.010
	10	14	1.44	2.400	1.509	1.450	2.316	1.239	1.188	2.286	1.134	1.097	0.051	0.415	0.000
	10	12	1.44	2.396	1.457	1.435	2.310	1.234	1.187	2.282	1.128	1.096	0.051	0.358	0.000
	10	10	1.44	2.390	1.391	1.402	2.308	1.232	1.185	2.267	1.126	1.091	0.056	0.287	0.015
	10	8	1.44	2.385	1.386	1.359	2.306	1.231	1.183	2.230	1.125	1.083	0.072	0.288	0.066
	10	6	1.44	2.381	1.323	1.298	2.305	1.217	1.181	2.215	1.119	1.081	0.078	0.223	0.089
	10	4	1.44	2.366	1.288	1.265	2.303	1.207	1.168	2.191	1.115	1.072	0.083	0.194	0.133
	10	2	1.44	2.323	1.264	1.236	2.267	1.192	1.150	2.125	1.109	1.061	0.098	0.179	0.194
	7	12	1.45	2.283	1.232	1.18	2.276	1.196	1.147	2.275	1.158	1.14	0.005	0.075	0.004
	7	10	1.45	2.276	1.23	1.177	2.27	1.195	1.146	2.256	1.157	1.132	0.009	0.077	0.017
	7	8	1.45	2.24	1.219	1.173	2.235	1.186	1.14	2.23	1.151	1.129	0.004	0.072	0.005
1-2	7	6	1.45	2.237	1.194	1.158	2.232	1.172	1.131	2.227	1.148	1.111	0.005	0.059	0.005
	7	4	1.45	2.219	1.186	1.132	2.211	1.15	1.11	2.207	1.134	1.081	0.005	0.073	0.002
	4	0	1.45	2.176	1.138	1.109	2.173	1.119	1.099	2.165	1.115	1.077	0.005	0.039	0.01
	7	12	1.49	2.405	1.332	1.305	2.362	1.154	1.125	2.221	1.120	1.117	0.086	0.209	0.191
	7	10	1.49	2.403	1.315	1.289	2.354	1.151	1.121	2.220	1.113	1.110	0.086	0.200	0.176
	7	8	1.49	2.369	1.301	1.277	2.319	1.138	1.112	2.218	1.110	1.105	0.070	0.190	0.122
2	7	6	1.49	2.367	1.300	1.275	2.267	1.135	1.111	2.190	1.104	1.099	0.084	0.196	0.057
	7	4	1.49	2.364	1.286	1.263	2.234	1.122	1.100	2.178	1.093	1.090	0.089	0.194	0.010
	4	0	1.49	2.357	1.274	1.246	2.225	1.111	1.090	2.167	1.076	1.078	0.092	0.200	0.012
	7	12	1.47	2.457	1.225	1.221	2.342	1.217	1.207	2.254	1.170	1.166	0.094	0.050	0.062
	7	10	1.47	2.425	1.236	1.224	2.339	1.216	1.208	2.253	1.163	1.158	0.079	0.067	0.076
3	7	8	1.47	2.424	1.224	1.215	2.306	1.215	1.206	2.248	1.150	1.140	0.081	0.071	0.019
	7	6	1.47	2.387	1.235	1.219	2.301	1.213	1.205	2.216	1.128	1.119	0.080	0.104	0.076
	6	4	1.47	2.373	1.248	1.215	2.297	1.211	1.203	2.188	1.123	1.093	0.088	0.134	0.120
	7	12	1.50	2.38	1.491	1.488	2.359	1.454	1.436	2.244	1.185	1.134	0.062	0.327	0.16
	7	10	1.50	2.38	1.489	1.485	2.346	1.449	1.427	2.242	1.13	1.125	0.063	0.372	0.134
4	7	8	1.50	2.325	1.478	1.476	2.297	1.443	1.43	2.24	1.127	1.123	0.039	0.363	0.066
	7	6	1.50	2.292	1.475	1.474	2.27	1.432	1.413	2.195	1.122	1.121	0.045	0.365	0.098
	7	4	1.50	2.227	1.474	1.469	2.2	1.402	1.383	2.175	1.115	1.113	0.024	0.375	0.022
	7	12	1.47	2.315	1.191	1.184	2.291	1.165	1.173	2.241	1.130	1.063	0.033	0.09	0.058
5	7	10	1.47	2.297	1.188	1.184	2.281	1.156	1.168	2.213	1.113	1.044	0.039	0.107	0.09

	7	8	1.47	2.280	1.183	1.179	2.270	1.156	1.157	2.206	1.120	1.050	0.034	0.094	0.087
	7	6	1.47	2.269	1.176	1.174	2.250	1.151	1.150	2.177	1.108	1.018	0.043	0.112	0.098
	7	4	1.47	2.258	1.174	1.172	2.226	1.140	1.090	2.148	1.111	1.020	0.053	0.107	0.1
	3	4	1.47	2.237	1.166	1.165	2.217	1.134	1.080	2.120	1.105	1.020	0.057	0.102	0.14
	7	12	1.61	2.639	1.384	1.382	2.626	1.371	1.373	2.414	1.187	1.122	0.098	0.219	0.31
	7	10	1.61	2.632	1.382	1.381	2.618	1.369	1.371	2.413	1.187	1.121	0.095	0.217	0.297
	7	8	1.61	2.619	1.370	1.368	2.615	1.370	1.369	2.371	1.154	1.114	0.11	0.23	0.382
6	7	6	1.61	2.618	1.369	1.368	2.615	1.356	1.357	2.364	1.152	1.112	0.113	0.231	0.398
	7	4	1.61	2.617	1.368	1.367	2.602	1.352	1.355	2.328	1.144	1.103	0.132	0.241	0.443
	3	4	1.61	2.616	1.365	1.366	2.577	1.284	1.305	2.287	1.133	1.078	0.154	0.262	0.466
	7	12	1.45	2.607	1.322	1.322	2.318	1.202	1.196	2.266	1.17	1.167	0.162	0.14	-0.08
	7	10	1.45	2.604	1.319	1.318	2.317	1.201	1.189	2.265	1.169	1.165	0.161	0.139	-0.08
	7	8	1.45	2.602	1.317	1.317	2.316	1.2	1.183	2.262	1.168	1.164	0.162	0.138	-0.08
7	7	6	1.45	2.594	1.308	1.306	2.273	1.192	1.181	2.254	1.165	1.163	0.162	0.131	-0.14
	7	4	1.45	2.591	1.307	1.308	2.272	1.191	1.18	2.253	1.164	1.162	0.161	0.131	-0.13
	3	4	1.45	2.562	1.304	1.305	2.25	1.179	1.173	2.248	1.163	1.161	0.149	0.13	-0.15
	7	12	1.45	2.284	1.168	1.163	2.245	1.126	1.123	2.222	1.099	1.098	0.028	0.065	0.013
	7	10	1.45	2.283	1.165	1.162	2.244	1.123	1.110	2.225	1.094	1.087	0.026	0.071	0.007
	7	8	1.45	2.281	1.163	1.160	2.245	1.115	1.110	2.217	1.094	1.078	0.029	0.073	0.021
8	7	6	1.45	2.280	1.161	1.159	2.211	1.104	1.087	2.174	1.053	1.029	0.05	0.122	0.017
	7	4	1.45	2.249	1.147	1.146	2.155	1.087	1.071	2.139	1.044	1.025	0.053	0.115	-0.02
	3	4	1.45	2.246	1.146	1.145	2.152	1.084	1.069	2.138	1.029	0.987	0.052	0.146	-0.03
	7	12	1.51	2.341	1.292	1.285	2.318	1.247	1.222	2.267	1.177	1.133	0.033	0.126	0.059
	7	10	1.51	2.337	1.305	1.311	2.300	1.254	1.260	2.257	1.139	1.120	0.036	0.167	0.041
	7	8	1.51	2.297	1.280	1.298	2.278	1.228	1.272	2.226	1.143	1.117	0.032	0.142	0.064
9	7	6	1.51	2.265	1.184	1.215	2.247	1.126	1.171	2.187	1.031	1.100	0.036	0.117	0.078
	7	4	1.51	2.240	1.177	1.152	2.194	1.137	1.126	2.155	1.025	0.910	0.04	0.24	0.032
	3	4	1.51	2.207	1.097	1.088	2.179	1.058	1.032	1.845	0.993	0.935	0.215	0.147	0.769
	7	12	1.45	2.260	1.366	1.284	2.247	1.167	1.179	2.238	1.098	1.155	0.010	0.235	0.006
	7	10	1.45	2.259	1.361	1.282	2.208	1.166	1.165	2.180	1.135	1.150	0.037	0.210	0.014
	7	8	1.45	2.252	1.357	1.277	2.207	1.165	1.165	2.175	1.098	1.146	0.036	0.231	0.023
	7	6	1.45	2.223	1.355	1.276	2.166	1.157	1.157	2.143	1.120	1.140	0.038	0.219	0.004
	7	4	1.45	2.390	1.229	1.232	2.225	1.135	1.178	2.190	1.080	1.156	0.095	0.104	-0.040
10	2	4	1.45	2.342	1.219	1.221	2.186	1.062	1.162	2.104	1.000	1.124	0.120	0.159	0.031
	10	12	1.45	2.447	1.376	1.278	2.264	1.266	1.246	2.251	1.168	1.180	0.091	0.187	-0.070
	10	10	1.45	2.446	1.370	1.286	2.263	1.263	1.248	2.247	1.165	1.168	0.092	0.190	-0.070
	10	8	1.45	2.440	1.368	1.285	2.263	1.258	1.254	2.245	1.164	1.167	0.091	0.189	-0.060
	10	6	1.45	2.438	1.354	1.273	2.257	1.252	1.246	2.215	1.163	1.166	0.106	0.176	-0.040
	10	4	1.45	2.430	1.340	1.271	2.254	1.244	1.245	2.207	1.161	1.165	0.106	0.164	-0.030

The length of the coal sample was measured with calipers before testing. During the test, it was corrected by the axial displacement gauge. The travel time of the first single arrival was picked with a high accuracy. Fig. 3 shows an example of waveforms and first arrival times for a sample taken at 45° to the bedding planes in group 6. With the first arrival time picked, the ultrasonic velocities for the eleven groups of samples can easily be calculated, as shown in Table 2.

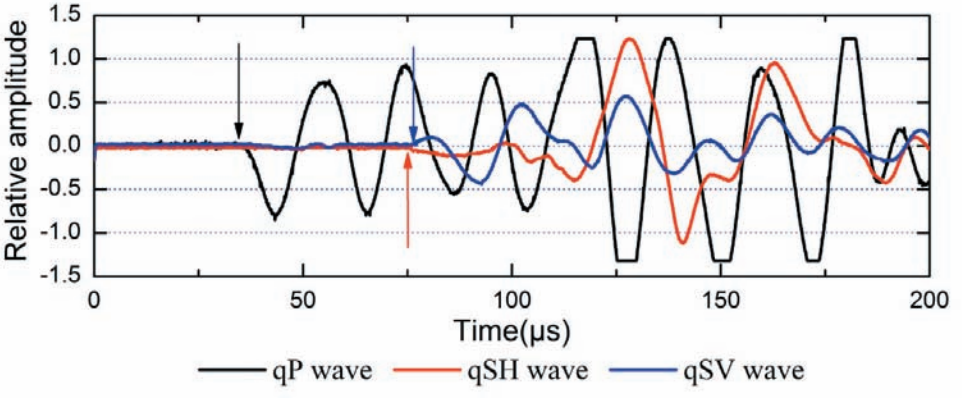

Fig. 3. Ultrasonic waveforms from sample 6, which was taken at 45° to the bedding planes.

Velocity error analysis

During testing, errors may be generated by instrumental or experimental factors, including instrument system errors, picking errors, and calculation and calibration errors. Hornby (1998) derived the following method to calculate the testing error:

$$\Delta V = \Delta L/(t_M - t_T) + L|\Delta t_M/(t_M - t_T)^2| + L|\Delta t_T/(t_M - t_T)^2| ,$$
$$\Delta V_{max} = \Delta L/(t_M - t_T) + 2L|\Delta t/(t_M - t_T)^2| , \quad (1)$$

where t_M is the traveltime of the first single arrival, Δt_M is the picking error, t_T is the docking time of the transducer, Δt_T is the docking time error, L is the length of the cylindrical coal sample, and ΔL is the length error. The sample taken at 45° to the bedding planes in group 6 is selected as an example. The value of $t_M - t_T$ for the qP wave is 38.10 μs, and 0.20 μs can be thought of as the maximum error for Δt_M and Δt_T, decided by the sampling interval (0.10 μs) and the picking error. The value of $t_M - t_T$ for the qSV wave is 73.20 μs. Since the first arrival of a single qS wave is harder to pick, here we evaluate Δt_M and

Δt_T as equal to 0.4 μs. The length of the sample is 99.1 mm after correction, and ΔL is 0.1 mm. Therefore, we obtain an absolute value for the qP wave velocity error of ± 18.9 m/s, which is 0.73% of V_P. Similarly, the error of the qSV wave velocity is ± 9.2 m/s, which is 0.68% of V_{SV}. Considering all the unavoidable factors mentioned above, the maximum errors for the qP wave and qSV wave velocities are estimated as less than 3%.

APPROXIMATE MODEL FOR THE CALCULATION OF THE ANISOTROPIC COEFFICIENTS FOR COAL SAMPLES

If there is no obvious variation in the transverse direction during deposition and limited tectonic movement during subsequent geological activities, the coal seam may have an integrated structure, and the anisotropy

(a) Bedding observation in coal blocks

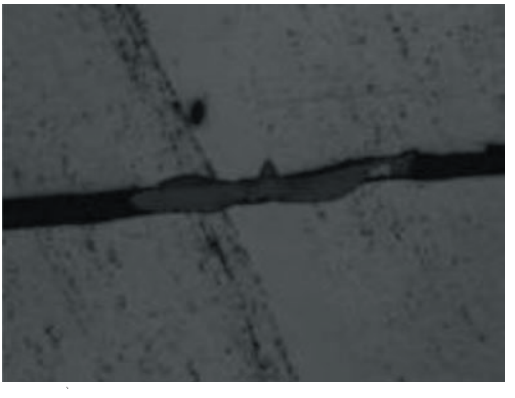

(b) Microscopic observation of coal sample bedding

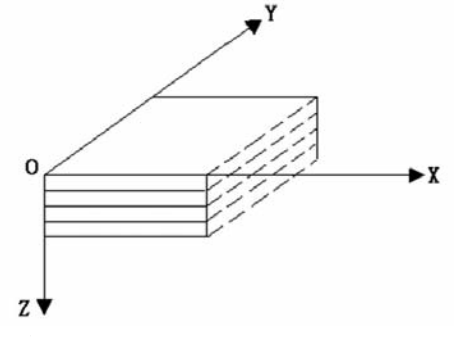

(c) VTI medium model

Fig. 4. VTI medium model approximation for coal samples.

will be predominantly controlled by the nearly horizontal bedding orientation, as in the VTI medium model (Dong, 2008). The horizontal bedding can be clearly observed in the original blocks and testing samples, and is completely or partially filled by calcite, as shown in Fig. 4(a). Under the microscope, the details and fillings of the bedding can be clearly seen, as shown in Fig. 4(b). Therefore, both the macroscopic and microscopic observations indicate that the test samples have the characteristics of VTI anisotropy.

To verify this assumption, a method proposed by Yu et al. (1993) is adopted, which maintains that the qS wave propagating along the symmetry axis of the VTI medium (perpendicular to the bedding planes) should satisfy the condition $V_{SH} \approx V_{SV}$ (Yu et al., 1993; Liu et al., 2012). As shown in Fig. 5, the maximum difference between V_{SH} and V_{SV} is about 6%, and most samples show a difference of about or less than 3%. Consequently, it is reasonable to assume that the test samples satisfy the condition $V_{SH} \approx V_{SV}$ for qS waves, and can be approximated as VTI media.

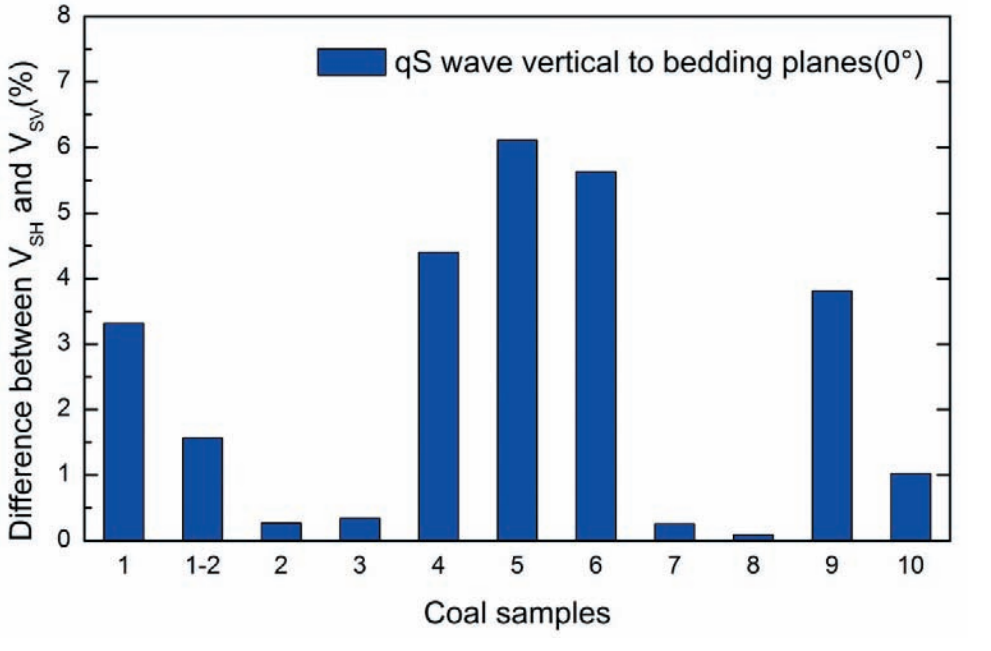

Fig. 5. Difference between V_{SH} and V_{SV} propagating along the symmetry axis in the VTI medium model.

For VTI media, three coefficients are generally used to describe the anisotropy of rocks (Thomsen, 1986). We calculate the following elastic constants:

$$C_{11} = \rho V_P^2(90°) \ ,$$

$$C_{13} = -C_{44} + \sqrt{[C_{11}+C_{44}-2\rho V_P^2(45°)][C_{33}+C_{44}-2\rho V_P^2(45°)]} \ ,$$

$$C_{33} = \rho V_P^2(0°) \ , \qquad (2)$$

$$C_{44} = \rho V_{SV}^2(90°) \ ,$$

$$C_{66} = \rho V_{SH}^2(90°) \ .$$

The anisotropic coefficients can be expressed as follows:

$$\varepsilon = (C_{11} - C_{33}) / 2C_{33} \ ,$$

$$\gamma = (C_{66} - C_{44}) / 2C_{44} \ , \qquad (3)$$

$$\delta = [(C_{13} + C_{44})^2 - (C_{33} - C_{44})^2] / 2C_{33}(C_{33} - C_{44}) \ .$$

The anisotropic coefficients are calculated according to eqs. (2) and (3), as shown in Table 2. Under a confining pressure of 12 MPa, the average values of $|\varepsilon|$, $|\gamma|$ and $|\delta|$ are 0.060, 0.175, and 0.080, respectively. Under a confining pressure of 4 MPa, the average values of $|\varepsilon|$, $|\gamma|$ and $|\delta|$ are 0.080, 0.176, and 0.093, respectively. Under both high and low confining pressures, the coal samples has weak anisotropy, and the average anisotropic coefficients satisfy the conditions $|\varepsilon| \leq 0.2$, $|\gamma| \leq 0.2$, and $|\delta| \leq 0.2$.

ULTRASONIC VELOCITY AND ANISOTROPIC COEFFICIENT ANALYSIS OF COAL SAMPLES

Ultrasonic velocity analysis

In this analysis, samples 5 and 8 are selected, with a test axial stress of 7 MPa and confining pressures ranging from 4 to 12 MPa. As shown in Fig. 6, the samples have the relationship V(90°) > V(45°) > V(0°) for both the qP and qS waves in all three directions. When the confining pressure is increased from 4 to 8 MPa for sample 5, the velocities increase by 1.0% - 2.7%, 0.8 - 1.2%, and 0.6 - 6.1% for the qP, qSH, and qSV waves, respectively, in all three directions. For sample 8, they increase by 1.4 - 4.2%, 1.4 - 4.7%, and 1.2 - 5.2%, respectively. This demonstrates that the velocity increases with confining pressures in samples 5 and 8 are significant, and sample 8 shows a larger percentage change than sample 5. Furthermore, when the confining pressure is increased from 8 to 12 MPa, the velocities for the qP, qSH, and qSV waves in all three directions increase by 0.9 - 1.6%, 0.7 - 0.9%, and 0.4 - 1.4%, respectively, for sample 5, and by 0 - 0.2%, 0.4 - 0.9%, and 0.2 - 1.8%, respectively, for sample 8. In contrast, above 8 MP, the velocities under higher confining pressures show no obvious variation and remain constant.

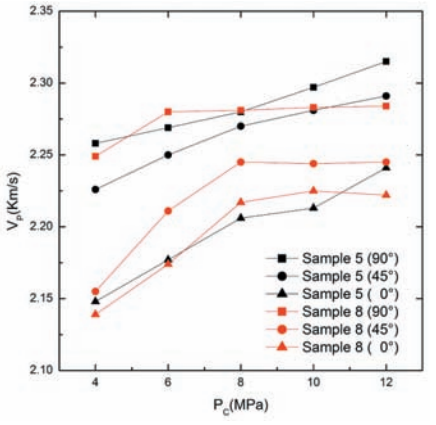

(a) Velocities of qP waves

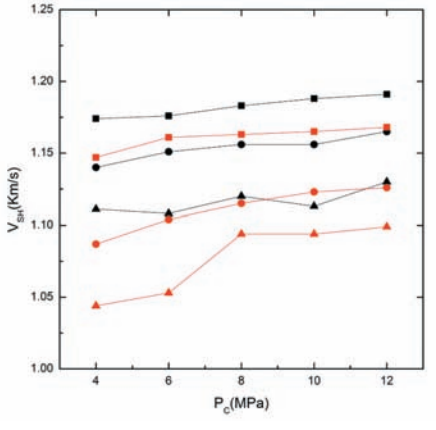

(b) Velocities of qSH waves

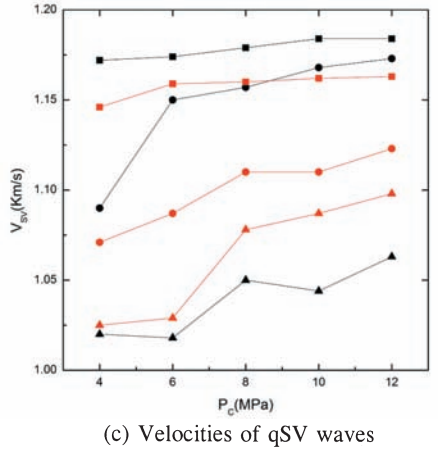

(c) Velocities of qSV waves

Fig. 6. Ultrasonic wave velocity variations for coal samples 5 and 8 under different confining pressures.

Some ultrasonic velocity tests on shale samples have shown that the axial stress may influence the velocity changes (Vernik and Nur, 1992; Kuila et al., 2011). Sample 1 is selected as an example using two significantly different axial stress settings of 4 MPa and 10 MPa. The qP wave velocities vary, as shown in Fig. 7. The velocities in all three directions become higher under greater axial stress, but still maintain the relationship V(90°) > V(45°) > V(0°) for each stress condition. When the axial stress is 10 MPa, the velocities of sample 1 only feature an obvious increase at confining pressures of less than 6 MPa, and change insignificantly at confining pressures above 6 MPa. Nevertheless, under an axial stress of 4 MPa, the velocities remain constant until the confining pressure reaches 10 MPa.

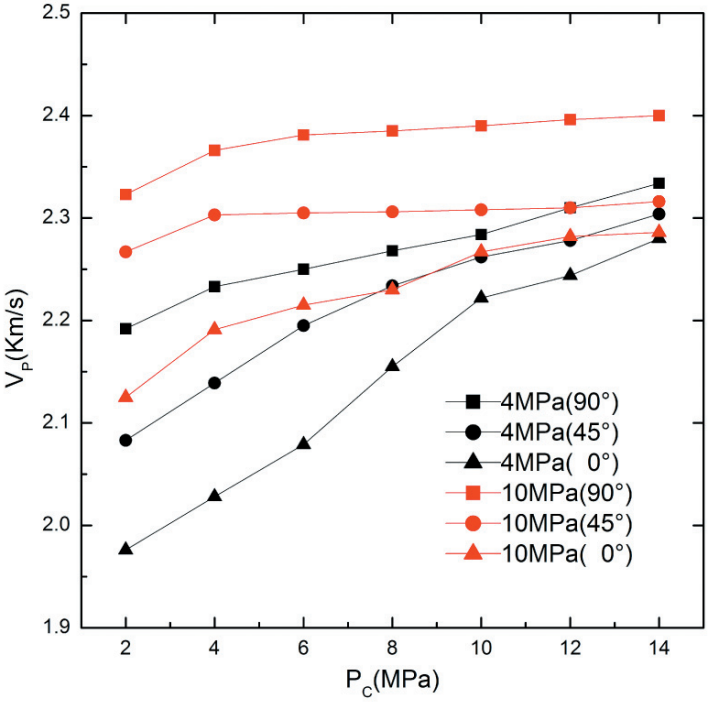

Fig. 7. Variation of qP wave velocities in coal sample 1 under different axial stresses.

Anisotropic coefficient analysis

We again select samples 5 and 8, with a test axial stress of 7 MPa and confining pressures ranging from 4 to 12 MPa, as example scenarios for this analysis. In Fig. 8, $\gamma > \varepsilon$ for nearly all the test samples, indicating stronger anisotropy for qS waves than qP waves. When the confining pressure is increased from 4 to 8 MPa, the anisotropic coefficients ε, γ and δ decrease by 0.019, 0.013, and 0.013, respectively, for sample 5, and 0.024, 0.042, and

−0.001, respectively, for sample 8. Additionally, when the confining pressure ranges from 8 to 12 MPa, they decrease by 0.001, 0.001, and 0.029, respectively, for sample 5, and 0.001, 0.008, and 0.008, respectively, for sample 8. The difference in the variation trends of the anisotropic coefficients between low and high confining pressures is significant. Both the ultrasonic velocities and anisotropic coefficients show similar characteristics with increasing confining pressures.

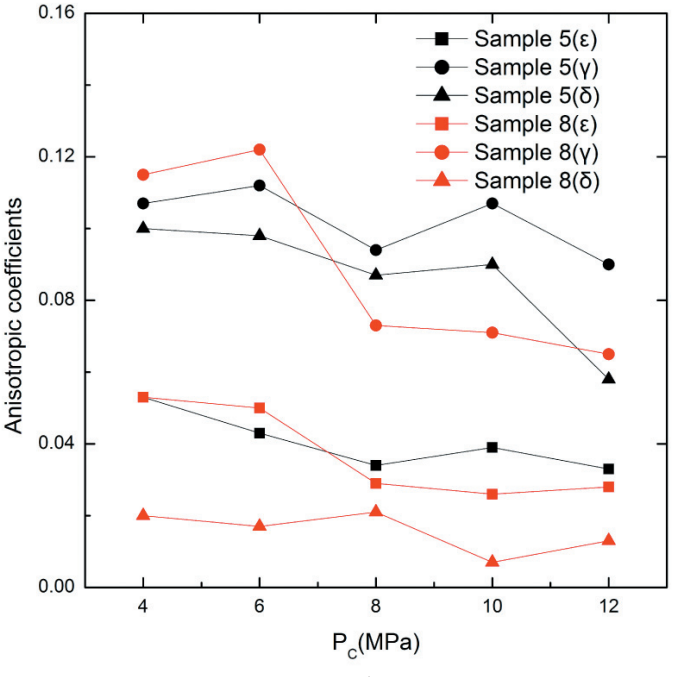

Fig. 8. Anisotropic coefficients of coal samples 5 and 8 under different confining pressures.

DISCUSSION

It is clear that the ultrasonic velocities in all the test samples increase with confining pressure, but the increase is not persistent and linear. In particular, there is a critical confining pressure below which a significant increase in the velocity is observed. This feature can be found in most of the samples tested in this study. However, the critical value may vary in many similar studies. For example, in this study, the critical value is 8 MPa (when the axial stress is 7 MPa), but in Yu et al. (1993) and Morcote et al. (2010), the critical confining pressures are 10 MPa and 5 MPa, respectively. Theoretically, this phenomenon may be related to the coal type and the axial stress setting. To test this hypothesis, we set two significantly different axial stresses for sample 1, 4 MPa and 10 MPa, which result in very different critical values, as seen in Fig. 7.

Furthermore, there is also a critical confining pressure value for the changes in the anisotropic coefficients, which approaches the critical value for the velocities under the same stress conditions.

The features discussed above may be related to dynamic changes in the microfractures and bedding in coal samples under confining pressures (Yu et al., 1993; Morcote et al., 2010). Under a low confining pressure, almost no disturbance occurs in the mineral matrix, but major closing of the microfractures and bedding occurs. Because microfractures are more compliant, the ultrasonic velocities increase, and anisotropic coefficients decrease significantly in sample 8. For sample 5, the same variation trend is seen, although the trend is weaker than for sample 8. After the confining pressure reaches the critical value, the elastic properties of the samples increase, as most of the microfractures are closed, corresponding to the conversion process from compaction to the elastic stage in the stress-strain curves (Morcote et al., 2010). Finally, under a high confining pressure, the ultrasonic velocities and anisotropic coefficients in sample 8 are essentially unchanged, while for sample 5, the variation is small because the limited inner microfracture development means that the velocities and anisotropy are mainly influenced by the bedding. Additionally, the ultrasonic velocities and anisotropy of the samples mainly reflect the properties of the mineral matrix, and the anisotropy is predominantly influenced by the orientation of the mineral compositions when under high stress.

CONCLUSIONS

In this study, we measure the ultrasonic velocities in anthracite samples collected from the Qinshui basin under triaxial stress conditions, describing in detail the collection and preparation of the coal samples, the test instruments, and the associated errors. We also calculate and analyze the ultrasonic velocities and anisotropic coefficients. Considering the depositional features of coal, combined with observations of the coal block and microscopic observations of the bedding, we find that the bedding is developed in a nearly horizontal direction, thus we approximate the samples as VTI media. Through an analysis of qS wave velocity variations, we confirm this assumption.

The ultrasonic velocities and anisotropic coefficients vary in a similar manner with increasing confining pressures, and there is a critical value for the confining pressure. The ultrasonic velocities increase, and the anisotropic coefficients decrease significantly when the confining pressure is below this critical value, corresponding to the dynamic process microfracture closure. Furthermore, as the microfractures begin to close, the elastic properties increase, and the variations in the velocities and anisotropic coefficients are small when the confining pressure is above the critical value. This critical value is affected by the axial stress and the coal type. This is illustrated

unambiguously by the significant variation of this value with different axial pressure levels. In summary, although the data and results obtained in this experiment are limited, we believe that they provide a reference for future studies in CBM rock physics.

ACKNOWLEDGEMENTS

The authors would like to acknowledge the A Project Funded by the Priority Academic Program Development of Jiangsu Higher Education Institutions (PAPD), the Jiangsu Natural Science Fund Project (No. BK20130201), and the Fundamental Research Funds for the Central Universities (No. 2012QNA62) for funding this research. We also thank the anonymous reviewers for their suggestions.

REFERENCES

Birch, F., 1960. The velocity of compressional waves in rocks to 10 kilobars. J. Geophys. Res., 65: 1083-1102.

Castagna, J.P., Batzle, M.L. and Kan, T.K., 1993. Rock physics: The link between rock properties and AVO response. In: Castagna, J.P. and Backus, M. (Eds.), Offset-Dependent Reflectivity-Theory and Practice of AVO Analysis. SEG, Tulsa, OK: 135-171.

Dong, S.H., 2008. Test on elastic anisotropic coefficients of gas coal. Chin. J. Geophys. (in Chinese), 51: 947-952.

Hornby, B.E., 1998. Experimental laboratory determination of the dynamic elastic properties of wet, drained shales. J. Geophys. Res., Solid Earth (1978-2012), 103(B12): 29945-29964.

Kuila, U., Dewhurst, D.N., Siggins, A.F. and Raven, M.D., 2011. Stress anisotropy and velocity anisotropy in low porosity shale. Tectonophysics, 503: 34-44.

Liu, W.L., 2009. Geophysical Response characteristics of coal bed methane. Lithol. Reserv., 21: 113-115.

Liu, Y.Y., Wang, Y. and Zhang, M.G., 2012. Discussion on the paper "Test on elastic anisotropic coefficients of gas coal". Progr. Geophys. (in Chinese), 27: 1832-1836.

Morcote, A., Mavko, G. and Prasad, M., 2010. Dynamic elastic properties of coal. Geophysics, 75(6): E227-E234.

Thomsen, L., 1986. Weak elastic anisotropy. Geophysics, 51: 1954-1966.

Vernik, L. and Nur, A., 1992. Ultrasonic velocity and anisotropy of hydrocarbon source rocks. Geophysics, 57: 727-735.

Wang, Y., Xu, X.K. and Zhang, Y.G., 2012. Characteristics of P-wave and S-wave velocities and their relationships with density of six metamorphic kinds of coals. Chin. J. Geophys., 55: 3754-3761. (In Chinese)

Wang, Z., 2002. Seismic anisotropy in sedimentary rocks, part 2: Laboratory data. Geophysics, 67: 1423-1440.

Yao, Q. and Han, D., 2008. Acoustic properties of coal from lab measurement. Expanded Abstr., 78th Ann. Internat. SEG Mtg., Las Vegas: 1815-1819.

Yu, G., Vozoff, K. and Durney, D.W., 1991. Effects of confining pressure and water saturation on ultrasonic compressional wave velocities in coals. Internat. J. Rock Mechan. Mining Sci. Geomechan. Abstr., 28: 515-522.

Yu, G., Vozoff, K. and Durney, D.W., 1993. The influence of confining pressure and water saturation on dynamic elastic properties of some Permian coals. Geophysics, 58: 30-38.